Geological Magazine

www.cambridge.org/geo

On the oxygenation of the Archaean and Proterozoic oceans

Amlan Banerjee[1], Mirosław Słowakiewicz[2,3] and Dilip Saha[1]

[1]Geological Studies Unit, Indian Statistical Institute, Kolkata 700108, India; [2]Faculty of Geology, University of Warsaw, Żwirki i Wigury 93, 02-089 Warszawa, Poland and [3]Kazan Federal University, Kremlovskaya 18, 420008 Kazan, Russia

Original Article

Cite this article: Banerjee A, Słowakiewicz M, and Saha D (2022) On the oxygenation of the Archaean and Proterozoic oceans. *Geological Magazine* **159**: 212–219. https://doi.org/10.1017/S0016756820001363

Received: 17 February 2020
Revised: 23 November 2020
Accepted: 25 November 2020
First published online: 23 December 2020

Keywords:
Archaean; Proterozoic; ocean; oxygenation; natural convection; forced convection; glaciation

Author for correspondence: Amlan Banerjee, Email: amlan@isical.ac.in

Abstract

Modern-day ocean circulation behaves as a complex forced convective system that is characterized by the decrease in water temperature but increase in water density with depth. The dissolved oxygen content – which initially decreases due to biological oxygen demand – also increases with depth. In contrast to the present-day scenario, we propose that during the Archaean and Proterozoic eons inverted profiles could have developed such that, with depth, ocean water temperature increased and density and dissolved oxygen decreased. These inverted temperature and density profiles resulted in palaeo-ocean circulation behaving as a free convective system. It is proposed that this free convection, which may have been stable, or chaotic and subject to secondary instabilities, hindered the deep oxygenation of the palaeo-ocean. It may not be coincidental that the great oxygenation event (GOE) and Huronian glaciations are contemporaneous, in a similar way that the Neoproterozoic oxygenation event (NOE) is known to have been associated with glaciations. The global-scale external forcing required to switch the natural convective system to its present-day configuration is suggested to have been associated with Neoproterozoic glaciations and the subsequent lowering of ocean water salinity that accompanied them. We propose that this inverted the ocean water density gradient, allowing the oxygenation of the oceans for the first time. It is beyond the scope of this work to model the complex natural convection system, but we hope that geophysicists and numerical modellers will quantitatively evaluate the hypothesis proposed here to validate or refute our proposition.

1. Introduction

The oxygenation mechanism of modern oceans is a well-defined physical process where atmospheric oxygen – absorbed into the water at the ocean–air interface – is transported to the depths by (1) complex convective mixing aided by eddy currents and turbulence, and (2) high-latitude externally forced subduction of cold, saline and oxygenated dense waters; such transportation has probably been underway since the Baykonurian glaciation during early Cambrian time (at 547 Ma; Germs & Gaucher, 2012). Scott *et al.* (2008) proposed that the deep oceans were oxygenated by 551 Ma, and that this was accompanied by a decrease in euxinic conditions within the water column. The air–water interaction over the convective ocean also enhanced air–water oxygen transfer. The present-day oceanic circulation is forced by wind stress, heat differentials, freshwater fluxes at the surface, tidal forcing, topography of the ocean floors and geothermal heat fluxes (Munk & Wunsch, 1998; Adcroft *et al.* 2001). Recently, Waldman *et al.* (2018) have proposed that the thermohaline circulation behaves as sinking rings of boundary currents proximal to high-latitude coastlines. On the other hand, the upwelling of the ocean water (in the Southern Hemisphere), which returns the deep waters to the surface, is mostly driven by the westerly winds (Toggweiler & Samuels, 1995; Marshall & Speer, 2012). The oxygenation of the ocean by absorption and convective mixing is strongly dependent on the thermal gradient of water and is expected to decrease with increasing temperature and ocean stratification. An increase in ocean stratification may inhibit convective mixing of oxygen-rich surface waters into the deeper ocean (Keeling *et al.* 2010) and may be particularly important in limiting the oxygenation of deep waters due to the dominant role of stratification in polar convection at the present day.

Convection is probably the most important physical process responsible for the oxygenation of the oceans and can be classified as natural (or free) or forced, depending on how the fluid motion is initiated. In natural convection, no external force is applied and fluid motion is caused by the buoyancy effect induced by density differences; it is more likely to be rapid with fluids with larger differences in density and lower viscosity. The denser fluids will sink, while less dense fluids will rise, causing net fluid movement and mass transfer; a familiar example of natural convection is the convection within the Earth's mantle which drives plate tectonics. Forced convection is the mechanism of mass and heat transfer through a fluid that is forced to flow by external influence unrelated to the fluid properties (e.g. along a hydraulic/topographic gradient

CAMBRIDGE UNIVERSITY PRESS

or by gravitational pull; Nield & Bejan, 2013). The term mixed convection is used when the fluid motion involves a combination of forced convection and natural convection caused by fluid density differences (Nield & Bejan, 2013).

Although the ocean is well oxygenated at present and the mechanism of ocean water oxygenation is well understood, the same cannot be said for all of geological history. Free oxygen was anything but plentiful (practically, there was no atmospheric oxygen) during the first half of Earth's 4.5 Ga history (Dutkiewicz *et al.* 2006; Holland, 2006). The amount of dissolved oxygen in the Earth's oceans at the beginning of or before the great oxidation event (GOE; *c.* 2.4–2.3 Ga) remains poorly understood, but it is thought the oceans were anoxic and sulphidic. It is generally agreed that global atmospheric oxygen concentrations that developed during the GOE remained more or less constant for the almost 2 Ga that followed before they increased to modern values in the late Neoproterozoic period or at the very beginning of the Cambrian Period (Lyons *et al.* 2014). It is hypothesized that throughout the Proterozoic Eon, long after the GOE, marine oxygen concentrations were likely to have been low and that euxinic (Canfield, 1998) or iron-rich anoxic conditions prevailed in the oceans (Scott *et al.* 2008; Lyons *et al.* 2009; Planavsky *et al.* 2011). Holland (2006) proposed that during 3.85–2.45 Ga surface and deep waters of the oceans were anoxic, but during 2.45–0.54 Ga surface ocean waters started to become mildly oxygenated while the deep oceans remained mostly anoxic. Anbar & Knoll (2002) proposed that for much of the Proterozoic Eon (2.45–0.54 Ga), the oceans were moderately oxic at the surface but anoxic and sulphidic at depth. Ostrander *et al.* (2019) similarly argued for the regional-scale episodic accumulation of dissolved oxygen in the oceans on continental shelves and margins during or before the GOE, but the extent of this oxygenation remains unclear. From 0.54 Ga onwards, at the beginning of the onset of the Phanerozoic Eon, ocean waters were completely oxygenated (Holland, 2006) and atmospheric oxygen concentrations began to increase up to their present-day values of 0.21 atm.

The oxidation state of the Proterozoic ocean between the GOE and Neoproterozoic oxidation event (NOE) and the timing of deep-ocean oxygenation have important implications for the evolutionary course of life on Earth, but still remains a matter of controversy. The aim of this study is to understand why a lag period of nearly 2.0 Ga was apparently necessary to oxygenate the palaeo-ocean by considering the physicochemical properties of Precambrian seawater, although it must be borne in mind that the available data is based on little more than broad estimates (Holland, 2003). Understanding the oxygenation of the palaeo-ocean is a daunting task and, at the best, we propose logical estimates here. The physical properties of the Archaean–Proterozoic oceans remain enigmatic and their palaeo-salinity, water temperature and chemistry are subject to much debate. To understand the oxygenation of the palaeo-ocean, estimates of the average depth and temperature of the waters as well as their salinity profile are required.

2. Methods of physical property estimation

Temperature and salinity strongly govern the oxygen solubility (Sharqawy *et al.* 2010) and ocean circulation patterns, but they are also largely unconstrained variables which have probably varied significantly over geological time. Here we discuss the methods applied in this study to estimate palaeo-depth profiles for temperature and salinity.

2.a. Palaeo-ocean depth

The depths of the Precambrian oceans are unknown. The preserved sedimentary sequences, even deep ones, are preserved on continental crust and the sedimentary facies interpretations are often very general. The qualifiers such as 'deep' and 'shallow' are difficult to quantify. As the relative bathymetry of palaeo-oceanic and continental basins is unknown in detail, we apply an average modern ocean depth of 4 km (Charette & Smith, 2010) for the purpose of numerical estimates as the representative depth for ancient oceans.

2.b. Temperature

The surface temperature of the Earth during the Archaean–Proterozoic eons is much debated. However, it is generally accepted that although the surface temperature was relatively higher compared with the present, it was less than the boiling point of water, ranging over 0–85 °C and was most likely between 55 and 85 °C (Knauth, 2005; Robert & Chaussidon, 2006; Krissansen-Totton *et al.* 2015; Marty *et al.* 2018). Ding *et al.* (2017) reported that a temperature range of 35–40 °C is more reasonable for the Archaean ocean, while the temperatures in the Proterozoic ocean are estimated to be in the range of 35–60 °C. Furthermore, Knauth (2005) suggested that the Palaeoproterozoic ocean surface temperature was approximately 40 °C. This elevated ocean surface temperature gradually decreased with time, to values (10–15 °C) similar to those of Phanerozoic time, as a result of the reduction of oceanic salinity associated with Neoproterozoic glaciations during 685–550 Ma.

Another constraint is provided by the estimated palaeo-heat flow and heat production data for Archaean–Proterozoic times. Data analysed from present-day Archaean–Proterozoic provinces are not sufficient to determine the palaeo-thermal regime (Mareschal & Jaupart, 2006), but it is generally accepted that the Proterozoic crust was thicker (*c.* 40–55 km) than during the Archaean Eon (*c.* 27–40 km; Durrheim & Mooney, 1991). For comparison, the present-day thickness of the continental crust is 30–70 km, while that of the oceanic crust is 6–12 km (Tewari *et al.* 2018). Reston & Morgan (2004) proposed that the geotherms in average Archaean continental crust were significantly elevated compared with modern values and at the end of the Archaean Eon, when crustal heat production was double that of the present. Mareschal & Jaupart (2006) estimated the average surface heat flow at the end of Archaean to be 45–90 mW m^{-2},while Lambert (1980) estimated that at 2.6 Ga the average equilibrium surface heat flow was *c.* 123 mW m^{-2} and that oceanic crust heat flow was 125 mW m^{-2}. In order to match this high heat flow, Lambert (1980) suggested that the oceanic crust would probably be composed of sub-hexagonal cells of dimension 130 × 500 km, and rimmed by upwelling materials and a central sink, or vice versa.

A thermal and salinity model of the palaeo-ocean is estimated here assuming the depth of the palaeobasin (z) as 4000 m (i.e. 4 km, as stated previously). For thermal modelling of the palaeo-ocean, two unconstrained parameters – ocean surface temperature and the basal heat flux (J_z) – are selected as variables for sensitivity analysis. The initial parameters of ocean temperature, that is, the temperature at the air–water interface (T_0) and the ocean bottom basal heat flux (J_z), are assumed to be 50 °C and 1.24 mW m^{-2}, respectively. Using Fourier's law, the temperature gradient ($m = dT/dz$) of the palaeo-ocean is estimated be J_z/κ, where κ, the thermal conductivity of ocean water, is 0.64 Wm^{-1} K^{-1} at $T = 50$ °C and present-day salinity (S_p) = 40‰ (Sharqawy *et al.* 2010). In the absence of free convection, the temperature distribution at any depth (z_i) is calculated using the linear expression $T_i = T_0 + mz_i$. For sensitivity analysis, the temperature of the air–

https://doi.org/10.1017/S0016756820001363 Published online by Cambridge University Press

water interface is adjusted in increments of 20 °C from 0 to 60 °C and the basal heat flux (J_z) is changed from an initial value of 1.24 mW m^{-2} to values of 0.0, 0.62 and 2.48 mW m^{-2}.

Note that the basal heat flux (J_z) values used in this study are much smaller than the value estimated by Lambert (1980). The J_z values used in this study are very conservative and chosen so that the ocean water temperature never attains boiling temperature. Using $J_z = 125$ mW m^{-2} would produce an elevated temperature gradient ($m = 0.19531$ K m^{-1}) that would raise the ocean water temperature at $z = 4$ km above boiling point, which is unlikely.

2.c. Salinity

The estimation of the salinity profile of the palaeo-ocean, another unconstrained parameter, is more complex than it may appear. Salinity of the ocean is a function of precipitation, temperature and ocean circulation; however, none of these variables are known for Archaean and Proterozoic times. Following Holland *et al.* (1986), De Ronde *et al.* (1997) and Knauth (2005), we estimated the ancient ocean water salinity (S_a) to be 1.2–2.0 times that of the present-day salinity (S_p), although Marty *et al.* (2018) suggested that the salinity of the Archaean–Proterozoic oceans was comparable to that of modern oceans.

2.d. Density

The density (ρ_w, kg m^{-3}) profile of the palaeo-ocean is estimated using the expression of Sharqawy *et al.* (2010):

$$\rho_w = (a_1 + a_2T + a_3T^2 + a_4T^3 + a_5T^4) + (b_1S_a + b_2S_aT + b_3S_aT^2 + b_4S_aT^3 + b_5{S_a}^2T^2),$$

which relates the density of seawater to temperature and salinity, where a_i ($i = 1, 2, 3 \ldots$) and b_i ($i = 1,2,3 \ldots$) are coefficients, S_a is the ancient ocean water salinity (g kg^{-1}), which is taken here to be $1.2 \times S_p$, and T is temperature (°C). Several density profiles are calculated by keeping the surface temperature fixed at 50 °C, but gradually increasing the basal heat flux (J_z) from 0.0 to 2.48 mW m^{-2} in the following increments: 0.0, 0.62, 1.24 and 2.48 mW m^{-2}, i.e. doubling the heat flux at each increment.

2.e. Dissolved oxygen

The dissolved oxygen (DO; μmol kg^{-1}) profile of the palaeo-ocean is estimated using the expression of Weiss (1970), which defines dissolved ocean water oxygen concentration as a function of temperature and salinity:

$$\ln C = A_1 + A_2(100/T) + A_3\ln(T/100) + A_4(T/100) + S_a[B_1 + B_2(T/100) + B_3(T/100)^2],$$

where, at standard temperature and pressure, C is the oxygen solubility (mL L^{-1} or mL kg^{-1}) from water saturated air at a total pressure of 1 atm; A and B are constants; T is the absolute temperature in degrees Kelvin (K); and S_a is ocean water salinity in per mil. Several dissolved oxygen profiles are calculated by fixing surface temperature at 50 °C, but increasing the basal heat flux (J_z) from 0.0 to 2.48 mW m^{-2} as previously, that is, in the increments: 0.0, 0.62, 1.24 and 2.48 mW m^{-2} and assuming $S_a = 1.2 \times S_p$.

2.f. Diffusion coefficient of oxygen

To the best of our knowledge there is no published data that provides diffusion coefficients for oxygen (D_{O2}) in water as a function of both temperature and salinity. We therefore used the experimental data of Ho *et al.* (1988), which correlated D_{O2} directly with salinity, and the empirical formulae of Han & Bartels (1996), which correlated D_{O2} as a dependent function of temperature as follows:

$$\log_{10}D = -4.706 + 903.6/T - (526.6/T)^2,$$

where D is in cm^2 s^{-1} and T is in degrees Kelvin.

The estimated D_{O2} profiles using the empirical relationships are calculated for ocean surface temperature fixed at 50 °C, basal heat flux (J_z) at 1.24 mW m^{-2} and an ocean water salinity of $S_a = 1.2 \times S_p$.

3. Results

3.a. Temperature profile

The results of the analyses show that adjusting the ocean surface temperatures and basal heat flux (J_z) vary the temperature profile of the ocean between reasonable limits.

3.a.1. Changing surface temperature only

In this numerical experiment, the ocean surface temperature is changed from 0 to 60 °C, keeping the ocean salinity ($S_a = 1.2 \times S_p$) and basal heat flux (1.24 mW m^{-2}) constant; the results are shown in Figure 1a (black lines). This scenario probably also imitates the change in polar to equatorial surface temperature. With a gradual increase in surface temperature from higher latitudes to lower latitudes, the results (in the absence of free convection) yield a progressive warming up of the ocean water. Ocean temperature, in the absence of free convection, also increases with depth irrespective of its latitudinal position, which is in contrast to the present-day temperature profile where temperatures decrease with depth (Fig. 1a). In addition, Figure 1a also illustrates that, for each increment in the surface temperature by 20 °C (i.e. $\Delta T = 20$ °C), the ocean temperature shifts systematically to the right (higher-temperature side) by the same ΔT from the previous estimate.

3.a.2. Changing basal heat flux only

The temperature profile of the ancient ocean will also change if the basal heat flux is altered but the effects of convection are excluded. Several sensitivity analyses are performed here by keeping the ocean surface temperature constant at 50 °C but doubling the basal heat flux from 0.62 to 1.24 and 2.48 mW m^{-2} (black dashed lines in Fig. 1b). For this scenario, an increase in the basal heat flux causes the temperature gradients to become less steep, but ocean water temperatures still increase with depth in contrast to modern-day temperature profiles (dashed black line in Fig. 1b). Note that when the basal heat flux is 0.0 mW m^{-2}, the ocean temperature remains fixed at 50 °C.

3.b. Salinity profile

The modern-day salinity profile (S_p) is shown as a solid black line in Figure 1c. Following Holland (1984), De Ronde *et al.* (1997) and Knauth (2005), the ancient ocean salinity (S_a), in calculations which exclude convection, will be 1.2–2 times modern-day salinity, that is, $S_a = 1.2 \times S_p$ (Fig. 1c). In this scenario the salinity profiles appear nearly constant at depths of *c.* 500 m depth.

https://doi.org/10.1017/S0016756820001363 Published online by Cambridge University Press

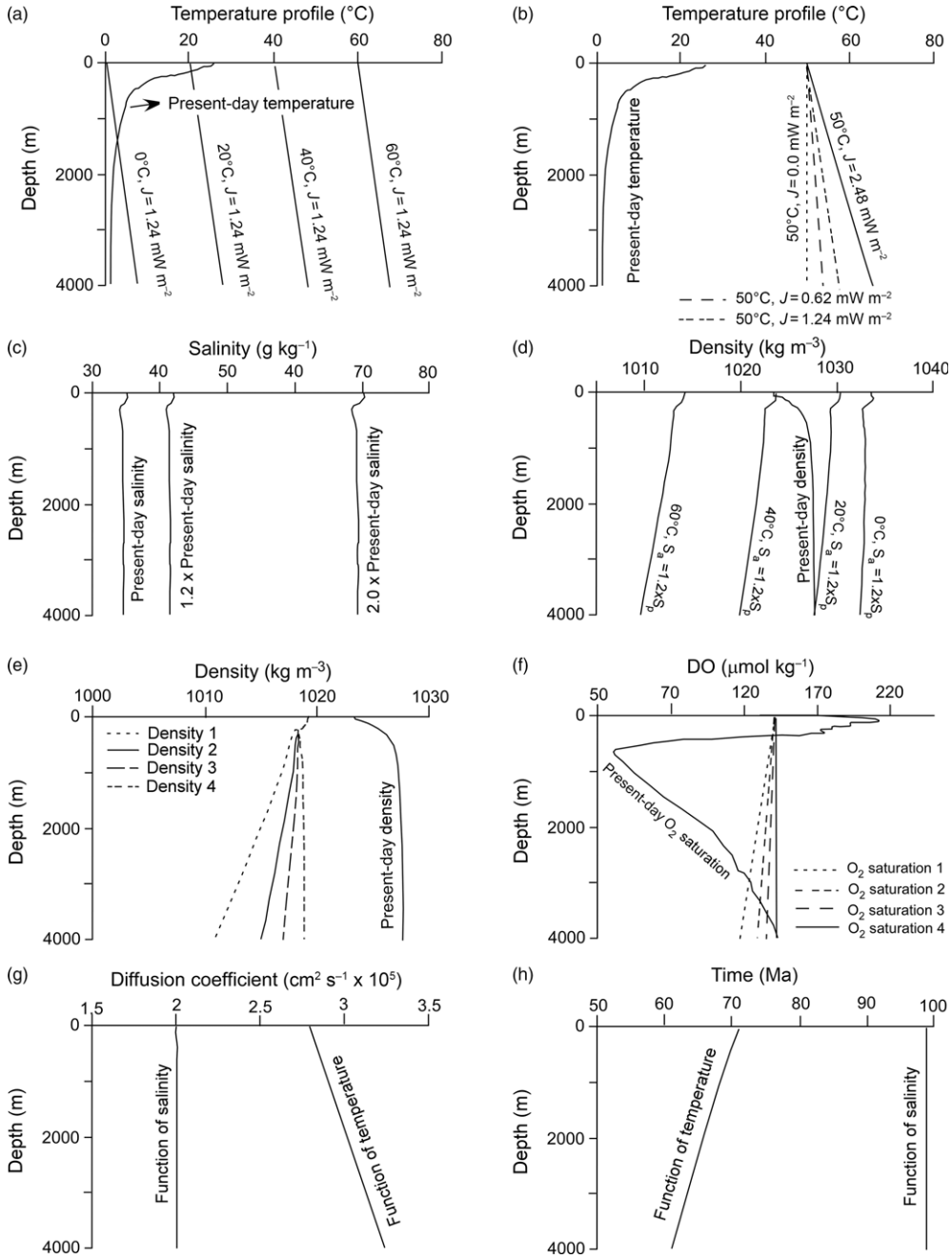

Fig. 1. (a) Calculated temperature profiles of the palaeo-ocean with variable surface temperature (0–60 °C) and constant basal heat flux ($J_z = 1.24$ mW m^{-2}) and salinity ($S_a = 1.2 \times S_p$). Temperatures at ocean bottom for each profile are 9.58, 29.58, 49.58 and 69.58 °C, respectively. The modern ocean temperature profile is also shown for comparison. This simulation could also represent the changes in palaeo-ocean surface water temperature from the polar regions towards the equatorial. (b) The calculated temperature profile of the palaeo-ocean when the surface temperature is fixed at a value of 50 °C but basal heat flux is varied. Where $J = 0$ mW m^{-2} the palaeo-temperature remains constant (this curve labelled $J = 2.48$ mW m^{-2}), whereas if $J > 0.0$ mW m^{-2}, temperatures increase with depth but the profiles become flatter. The ocean bottom temperature is 50, 53, 57 and 65 °C for corresponding J values of 0.0, 0.62, 1.24 and 2.48 mW m^{-2}, respectively; for comparison, the modern ocean temperature profile is also shown. Both scenarios in (a) and (b) demonstrate that the temperature of the palaeo-ocean increases with depth. (c) The salinity profile of the present-day ocean along with the salinity estimates for ancient oceans. Note that palaeo-salinity is increased systematically by either 1.2 or 2 times modern-day salinity and, for practical purposes, remains nearly constant below depths of 500 m. (d) Calculated density profiles of the palaeo-ocean with surface temperature (0–60 °C), and constant basal heat flux ($J = 1.24$ mW m^{-2}) and salinity ($S_a = 1.2 \times S_p$). (e) Estimated density profiles of the palaeo-ocean with the present-day ocean density profile. The palaeo-density profiles are calculated for a specific salinity value ($S_a = 1.2 \times S_p$), a surface temperature of 50 °C and basal heat flux of 0.0, 0.62, 1.24 and 2.48 mW m^{-2}. Note that the palaeo-ocean water was less dense than modern ocean water, and shows a density inversion. (f) The dissolved oxygen in the palaeo-ocean as a function of variable ocean water temperature as calculated in (b), and with a salinity profile of $S_a = 1.2 \times Sp$. The calculations show that, even for a warm and saline ocean, the calculated dissolved oxygen values in the palaeo-ocean are within the limits of present-day values. (g) Diffusion coefficient (cm^2 s$^{-1} \times 10^{-5}$) of oxygen as a function of salinity and temperature. The oxygen diffusion constant is not affected by salinity changes, whereas it increases progressively with increasing depth and temperature. (h) Time required for oxygen to diffuse through the ocean water as a function of temperature and salinity. The salinity of ocean water is the major controlling factor for oxygen diffusion.

https://doi.org/10.1017/S0016756820001363 Published online by Cambridge University Press

3.c. Density profile

The palaeo-ocean density profiles (in the absence of free convection) (Fig. 1d) are calculated here by changing surface water temperature (and accounting for latitudinal effects) using salinity values which are 1.2 times ($S_a = 1.2 \times S_p$) those of the present day, and keeping the basal heat flux (1.24 mW m^{-2}) constant. The estimated density profiles (Fig. 1d) suggest that, irrespective of surface water temperature, palaeo-ocean density decreases with depth in contrast to the modern density profile (black line in Fig. 1d), which implies that palaeo-ocean waters become more dense at shallower depths. Results also suggest that palaeo-ocean waters at higher latitudes will be considerably more dense than waters at lower latitudes (Fig. 1d). According to our calculations, the density of palaeo-ocean waters will be strongly dependent on salinity. If the surface temperature and basal heat flux (1.24 mW m^{-2}) are constant, the estimated density of the palaeo-ocean will be higher than that of the present-day ocean if the surface temperature is < 40 °C, and will be less when the surface water temperature is > 40 °C. Increasing the palaeo-salinity values to double that of present-day salinities ($S_a = 2.0 \times S_p$) will elevate palaeo-ocean densities such that the entire ocean waters, irrespective of their surface temperature, will become denser than those of present-day oceans. In contrast, if the palaeo-salinity is similar to that of the present-day value (i.e. $S_a = S_p$), then the palaeo-ocean density, irrespective of its surface temperature, will be less dense than that of present-day oceans. Density calculations also show that the density difference ($\Delta\rho = \rho_{max} - \rho_{min}$) of the palaeo-ocean will increase with ocean surface temperature (Fig. 1d). Density contrasts increase when ocean surface temperatures increase, and decrease as ocean surface temperatures are reduced. For example, at 0 °C palaeo-ocean surface temperature the density difference ($\Delta\rho$) is 1.57 kg m^{-3} for $S_a = 1.2 \times S_p$ and 2.38 kg m^{-3} for $S_a = 2.0 \times S_p$; at 60 °C, $\Delta\rho$ is 5.65 kg m^{-3} for $S_a = 1.2 \times S_p$ and 6.0 kg m^{-3} for $S_a = 2 \times S_p$. The sensitivity study suggests that, irrespective of the salinity of the palaeo-ocean, density decreases with increasing ocean surface temperature while density differences decrease as ocean surface temperatures decrease.

The effect of basal heat flux on the palaeo-density profiles in the absence of free convection are also calculated here for a specific salinity value ($S_a = 1.2 \times S_p$), and at a specific surface temperature of 50 °C using values of basal heat flux that are increased incrementally from 0.0, 0.62, 1.24 to 2.48 mW m^{-2}. With an increase in basal heat flux the slope of the estimated palaeo-density profiles become less steep, suggesting that the oceans become less dense, at shallower depths.

3.d. Dissolved oxygen profile

Unlike modern-day dissolved oxygen concentrations, calculations which exclude convection show a decrease in dissolved oxygen for the palaeo-oceans with increasing depth and temperature if salinity is kept constant ($S_a = 1.2 \times S_p$; Fig. 1f). It should be noted that the calculated values are an estimate of the maximum dissolved oxygen concentration, which, in turn, is a function of the temperature and salinity of the palaeo-ocean. In fact, the concentration of the dissolved oxygen could be low or null depending on the availability of free atmospheric oxygen.

3.e. Diffusion coefficient of oxygen

The estimated diffusion coefficient profiles of oxygen (D_{O2}) in the absence of free convection are shown in Figure 1g, and clearly show that the estimated D_{O2} values (solid black line in Fig. 1g) do not change with salinity, remaining constant at *c.* 2.0 × 10^{-5} cm^2 s^{-1}, whereas with an increase in water temperature from 40 °C at the surface to 50 °C at the bottom, D_{O2} increases by a factor of 1.2 from 2.8 to 3.35 (× 10^{-5} cm^2 s^{-1}) (black line in Fig. 1g).

For a palaeo-ocean of 4000 m depth, the time t needed for the dissolved oxygen to reach the ocean bottom is inversely proportional to the oxygen diffusion coefficient (D, m^2 s^{-1}), that is, $t = z^2/4D$, where z is depth in metres. This was calculated as a function of temperature and salinity, and the results (Fig. 1h) suggest that, with an increase in palaeo-ocean water temperature from 40 to 50 °C, the D_{O2} values increase. It would take *c.* 60–70 Ma for the oxygen to reach the ocean bottom with a depth of 4000 m and, if $S_a = 1.2 \times S_p$, it would take significantly longer (*c.* 100 Ma). This sensitivity study clearly demonstrates that the transport of dissolved oxygen by diffusion alone is strongly dependent on salinity.

4. Discussion

Geochemical data suggest that atmospheric oxygenation occurred in two broad steps near the beginning (GOE) and end (NOE) of the Proterozoic Eon (Scott *et al.* 2008) with a gap of nearly 2000 Ma. The oxidation state of the Archaean–Proterozoic oceans prior to the NOE and the timing of deep-ocean oxygenation have important implications for the evolutionary course of life on Earth, but remain poorly known (Scott *et al.* 2008). Anbar & Knoll (2002) proposed that anoxic oceans persisted for some 2000 Ma of early history, followed by intermediate oceans (oxic at the surface, but anoxic and sulphidic at depth) for more than 1000 Ma and originated some time after *c.* 1800 Ma. Oxic oceans, similar to those of the present day, then followed. In general, it is accepted that during 3.85–2.45 Ga ocean waters were completely anoxic; after this, during 2.45–0.54 Ga, they became mildly oxic although the deep oceans remained mostly anoxic and sulphidic. This profile is explained by a combination of low P_{O2} (< 0.07 atm) and reduced biological activity compared with modern-day oceans (Anbar & Knoll, 2002). To explain this ocean water oxic–sulfidic conundrum, a simple physical model is proposed that is independent of external chemical or biological forcing. The model presented here takes into account three important physical factors – ocean surface temperature, heat flux from the ancient oceanic lithosphere and ocean salinity profiles – to explain the dissolved oxygen profile of the palaeo-ocean water. Note that the feedback or regulatory mechanisms for biotic production of the dissolved oxygen in the ancient oceans is unknown and not considered here, but the elevated salinity and higher temperature of the palaeo-ocean would probably limit biotic activity.

The results, which exclude convection, suggest two probabilities. In the first scenario, if the temperature and the salinity of the ancient ocean remained constant, then the density and dissolved oxygen concentration would also remain constant and the ancient ocean would behave like a steady-state system, where $\partial(T,\ S,\ DO,\ D_{O2})/\partial t = 0$, that is, it will remain unchanged through time.

The system will behave differently when the palaeo-ocean temperature profile has a positive thermal gradient as is proposed here; this, along with elevated salinity, causes the density gradient as well as the dissolved oxygen concentration profile within the oceans to be negative. The negative oxygen concentration gradient would have inhibited the diffusion of oxygen down into the deep ocean. This would explain why the regional-scale accumulation of dissolved oxygen in the palaeo-oceans occurred only along the shallow continental shelves and margins at depths of a few hundred metres,

https://doi.org/10.1017/S0016756820001363 Published online by Cambridge University Press

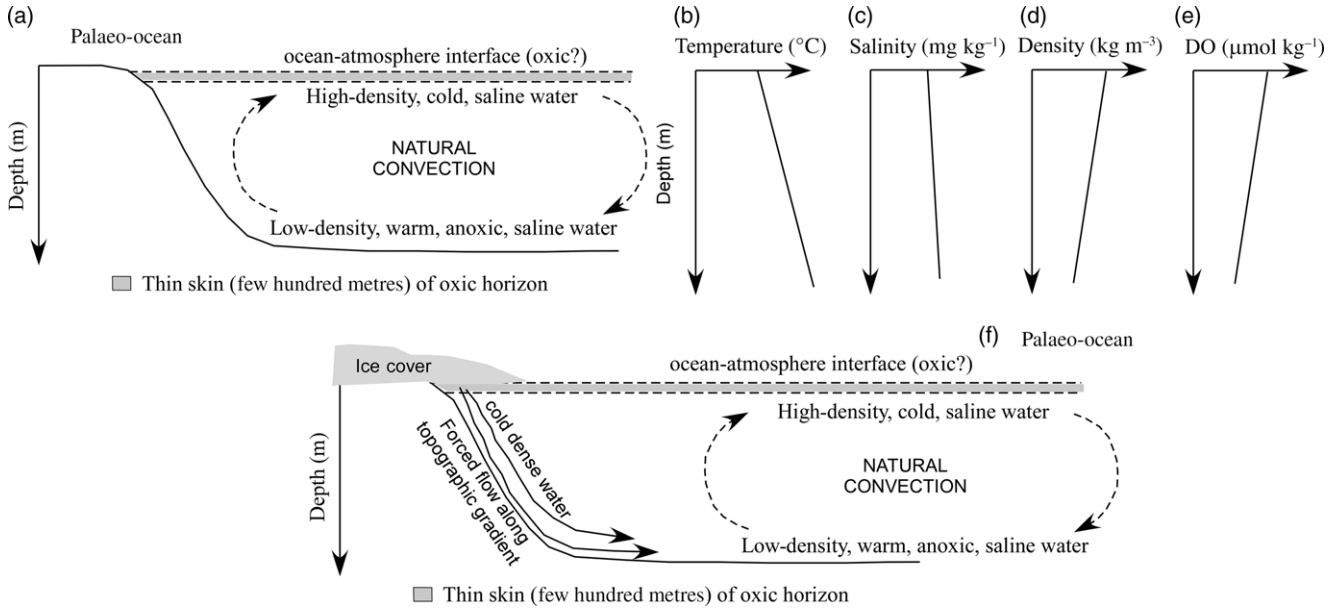

Fig. 2. (a) Proposed model based on (b) estimated palaeo-ocean water temperature, (c) salinity, (d) density and (e) dissolved oxygen profiles. The model suggests an inverted profile where hot and lower-density water resides at the bottom and the cold and dense water resides at or near the surface, contrary to the modern-day situation. Due to this density and thermal inversion, a natural convective circulation will take over as the preferred circulation system. This will lead to a regional-scale flow pattern that may either be stable or else fall prey to a host of secondary instabilities or become chaotic. Also note that, as a result of natural convection, dissolved oxygen in the water cannot diffuse to the bottom because of the temperature barrier as well as the higher salinities existing there. This will lead to a thin oxygenated surficial layer in the basin and anoxic conditions at depth. (f) The advent of Neoproterozoic glaciations will have allowed sustained forced flow (in the absence of buoyancy forces) of dense, cold oxygenated waters from the ocean margins along the topographic gradient to the ocean floor, and will have acted against natural convection by gradually weakening it and eventually causing the system to switch to its present configuration.

and certainly less than 1000 m (Fig. 2). The extent of this shallow oxygenation is strongly correlated with palaeo-ocean temperature and salinity. A depth of less than a few hundred metres is also the penetration depth of wind-driven surface currents and waves, which probably mixed the upper layers (few hundred metres depth) of the palaeo-ocean. On the other hand, a negative density gradient for the palaeo-ocean implies that the ocean bottom contained low-density, hot, anoxic and saline waters overlain by relatively cold, dense waters. Due to this density inversion it is expected that the palaeo-ocean would have experienced natural convection where the less-dense hot, saline and anoxic bottom waters would have been subject to upwelling due to the negative density gradient (Fig. 2). This convective fluid motion would also transport heat through the water column. The physical model presented here supports the models of Canfield (1998) who pointed out that the supply of oxygen to the deep oceans during this period was almost certainly much lower than today, if not absent.

Numerical estimates which include latitudinal temperature distribution (Fig. 1a, d) suggest that, irrespective of the salinity effect, palaeo-ocean density decreased with an increase in surface temperature while density differences ($\Delta\rho = \rho_{max} - \rho_{min}$) decrease with a reduction in surface temperature. This implies that free convection will be more vigorous in the equatorial regions where the surface temperature and the density differences between the top and bottom waters will be higher compared with the polar regions, where palaeo-ocean temperatures were near zero and there were minimal density differences between top and bottom waters. This would have led to near stagnation of the polar palaeo-ocean, with only sluggish natural convection. The palaeo-ocean water density differential between the equatorial and polar regions would probably impose a bottom flow from the high-density polar regions to the low-density equatorial regions. However, the distance that this bottom flow would be able to travel in an equatorial direction is debatable, and most probably would be limited by the upwelling caused by natural convection.

The mathematical expression of fluid movement by natural convection was first proposed by Bénard (1900) and modified by Rayleigh (1916) in his classic paper. Their work proposed that an initially motionless fluid layer becomes unstable as a result of the flow perturbations of fluids with sufficiently large temperature differences (Rayleigh–Bénard convection). Hot fluid near the ocean bottom expands and becomes less dense than the fluid above, so it rises, cools and returns in an overturning flow. This upwelling movement of fluid is opposed by the viscosity of the fluid and the tendency for thermal diffusion to smooth out temperature gradients. The vigour of thermal convection can be described by the Rayleigh number (R), which is a function of temperature gradient ($\beta = -dT/dz$), acceleration due to gravity (g, m s^{-2}), the coefficient of thermal expansion (α, $°C^{-1}$), depth of the system (z, m), thermal diffusivity (κ, m^2 s^{-1}) and kinematic viscosity (ν, m^2 s^{-1}). The Rayleigh number represents the ratio of the destabilizing buoyancy force relative to the stabilizing viscous force. The flow pattern may be stable, or it may fall prey to a host of secondary instabilities or become chaotic. This strong natural convection will probably be superimposed by a weak bottom flow from the polar regions towards the equator. This is in contrast with the modern-day ocean circulation where, with depth, the ocean water temperature decreases and salinity increases, making the seawater denser at the bottom and less dense at the top.

To change the ocean circulation from natural convection (with a weak bottom flow component) to its present condition, severe and sustained external thermal perturbation was required. We propose that the Neoproterozoic glaciation events – the Sturtian (715–680 Ma; Kendall *et al.* 2006), Marinoan (650–635 Ma;

https://doi.org/10.1017/S0016756820001363 Published online by Cambridge University Press

Shields, 2008), Gaskiers (*c.* 580 Ma; Pu *et al.* 2016) and Baykonurian (*c.* 547 Ma; Germs & Gaucher, 2012) glaciations – were the factor that switched the ocean circulation from natural convection to forced convection, and which was sustained in the later times by Phanerozoic glaciations during the Late Ordovician Epoch (Finnegan *et al.* 2011), during the Mississippian and Pennsylvanian periods (Karoo glaciations) and during the late Cenozoic Era.

5. Conclusions

The natural convection of the ancient ocean will probably have operated for *c.* 2000 Ma until powerful external forces and/or perturbations forced the system to switch and start to behave like a forced-convection system. The required perturbation is suggested to have been the lowering of ocean water salinity together with major cooling associated with the Neoproterozoic glaciations, along with the gradual cooling of the Earth (reducing the basal heat flux). This probably allowed the system to permanently change to its stable modern-day configuration. Once this physical condition was attained, the dissolved oxygen concentration in the ocean started to increase for the first time. It is worth mentioning here that the GOE and Huronian glaciation were nearly contemporaneous and followed by a protracted time interval (*c.* 2000 Ma) with greenhouse conditions (Tang & Chen, 2013) that lasted until the next Neoproterozoic glaciation. We are unable to model the proposed natural convection of the ancient ocean; for even the simplest thermal convection, problems governing the equations are highly complex and beyond the scope of this work. We encourage the numerical modellers to validate or refute our reasoning.

Acknowledgements. This work was supported by and contributes to the Proterozoic research programme of the Indian Statistical Institute. We also thank Mike Mawson for his remarks and linguistic correction. We also appreciate the constructive and helpful suggestions of three anonymous reviewers. This study was also supported by the Russian Government Programme of Competitive Growth of the Kazan Federal University.

Declaration of interest. None.

References

Adcroft A, Scott JR and Marotzke J (2001) Impact of geothermal heating on the global ocean circulation. *Geophysical Research Letters* **28**, 1735–8.

Anbar AD and Knoll AH (2002) Proterozoic ocean chemistry and evolution: a bioinorganic bridge? *Science* **297**, 1137–42.

Bénard H (1900) Les tourbillons cellulaires dans une nappe liquide. *Revue Générale des Sciences Pures et Appliquées* **11**, 1261–71, 1309–28.

Canfield DE (1998) A new model for Proterozoic ocean chemistry. *Nature* **396**, 450–3.

Charette M and Smith W (2010) The volume of Earth's ocean. *Oceanography* **23**, 112–4.

De Ronde CEJ, Channer DMdeR, Faure K, Bray CJ and Spooner ETC (1997) Fluid chemistry of Archaean seafloor hydrothermal vents: implications for the composition of circa 3.2 Ga seawater. *Geochimica et Cosmochimica Acta* **61**, 4025–42.

Ding TP, Gao JF, Tian SH, Fan CF, Zhao Y, Wan DF and Zhou JX (2017) The δ^{30}Si peak value discovered in middle Proterozoic chert and its implication for environmental variations in the ancient ocean. *Scientific Reports* **7**, 1–15.

Durrheim RJ and Mooney WD (1991) Archaean and Proterozoic crustal evolution: evidence from crustal seismology. *Geology* **19**, 606–9.

Dutkiewicz A, Volk H, George SC, Ridley J and Buick R (2006) Biomarkers from Huronian oil-bearing fluid inclusions: an uncontaminated record of life before the Great Oxidation Event. *Geology* **34**, 437–40.

Finnegan S, Bergmann K, Eiler JM, Jones DS, Fike DA, Eisenman I, Hughes NC, Tripati AK and Fischer WW (2011) The magnitude and duration of Late Ordovician–Early Silurian glaciation. *Science* **331**, 903–6.

Germs GJB and Gaucher C (2012) Nautre and extent of a late Ediacaran (ca. 547 Ma) glacigenic erosion surface in Southern Africa. *South African Journal of Geology* **115**, 91–102.

Han P and Bartels DM (1996) Temperature dependence of oxygen diffusion in H_2O and D_2O. *The Journal of Physical Chemistry* **100**, 5597–602.

Ho CS, Ju L-K, Baddour RF and Wang DIC (1988) Simultaneous measurement of oxygen diffusion coefficients and solubilities in electrolyte solutions with a polarographic oxygen electrode. *Chemical Engineering Science* **43**, 3093–107.

Holland HD (1984) *The Chemical Evolution of the Atmosphere and Oceans*. Princeton: Princeton University Press, 598 p.

Holland HD (2003) 6.21. The geologic history of seawater. In *Treatise on Geochemistry* (eds HD Holland and KK Turekian), pp. 583–625. Amsterdam: Elsevier.

Holland HD (2006) The oxygenation of the atmosphere and oceans. *Philosophical Transactions of the Royal Society B: Biological Sciences* **361**, 903–15.

Holland HD, Lazar B and McCaffrey M (1986) Evolution of the atmosphere and oceans. *Nature* **320**, 27–33.

Keeling RF, Körtzinger A and Gruber N (2010) Ocean deoxygenation in a warming world. *Annual Review of Marine Science* **2**, 199–229.

Kendall B, Creaser RA and Selby D (2006) Re-Os geochronology of postglacial black shales in Australia: constraints on the timing of "Sturtian" glaciation. *Geology* **34**, 729–32.

Knauth LP (2005) Temperature and salinity history of the Precambrian ocean: implications for the course of microbial evolution. *Palaeogeography, Palaeoclimatology, Palaeoecology* **219**, 53–69.

Krissansen-Totton J, Buick R and Catling DC (2015) A statistical analysis of the carbon isotope record from the Archaean to Phanerozoic and implications for the rise of oxygen. *American Journal of Science* **315**, 275–316.

Lambert RStJ (1980) The thermal history of the Earth in the Archaean. *Precambrian Research* **11**, 199–213.

Lyons TW, Anbar AD, Severmann S, Scott C and Gill BC (2009) Tracking euxinia in the ancient ocean: a multiproxy perspective and Proterozoic case study. *Annual Review of Earth and Planetary Sciences* **37**, 507–34.

Lyons TW, Reinhard CT and Planavsky NJ (2014) The rise of oxygen in Earth's early ocean and atmosphere. *Nature* **506**, 307–15.

Mareschal J-C and Jaupart C (2006) Archaean thermal regime and stabilization of the cratons. In *Archaean Geodynamics and Environments* (eds K Benn, J-C Mareschal and KC Condie), pp. 61–73. Washington: American Geophysical Union (AGU), Geophysical Monograph Series, 164.

Marshall J and Speer K (2012) Closure of the meridional overturning circulation through Southern Ocean upwelling. *Nature Geoscience* **5**, 171–80.

Marty B, Avice G, Bekaert DV and Broadley MW (2018) Salinity of the Archaean oceans from analysis of fluid inclusions in quartz. *Comptes Rendus Geoscience* **350**, 154–63.

Munk W and Wunsch C (1998) Abyssal recipes II: energetics of tidal and wind mixing. *Deep Sea Research Part I: Oceanographic Research Papers* **45**, 1977–2010.

Nield DA and Bejan A (2013) *Convection in Porous Media* 4th ed., New York: Springer-Verlag, 778 pp.

Ostrander CM, Nielsen SG, Owens JD, Kendall B, Gordon GW, Romaniello SJ and Anbar AD (2019) Fully oxygenated water columns over continental shelves before the Great Oxidation Event. *Nature Geoscience* **12**, 186–91.

Planavsky NJ, McGoldrick P, Scott CT, Li C, Reinhard CT, Kelly AE, Chu X, Bekker A, Love GD and Lyons TW (2011) Widespread iron-rich conditions in the mid-Proterozoic ocean. *Nature* **477**, 448–51.

Pu JP, Bowring SA, Ramezani J, Myrow P, Raub TD, Landing E, Mills A, Hodgin E and Macdonald FA (2016) Dodging snowballs: geochronology of the Gaskiers glaciation and the first appearance of the Ediacaran biota. *Geology* **44**, 955–8.

Rayleigh L (1916) LIX. On convection currents in a horizontal layer of fluid, when the higher temperature is on the under side. *The London, Edinburgh, and Dublin Philosophical Magazine and Journal of Science* **32**, 529–46.

https://doi.org/10.1017/S0016756820001363 Published online by Cambridge University Press

Reston TJ and Morgan JP (2004) Continental geotherm and the evolution of rifted margins. *Geology* **32**, 133–6.

Robert F and Chaussidon M (2006) A palaeotemperature curve for the Precambrian oceans based on silicon isotopes in cherts. *Nature* **443**, 969–72.

Scott C, Lyons TW, Bekker A, Shen Y, Poulton SW, Chu X and Anbar AD (2008) Tracing the stepwise oxygenation of the Proterozoic ocean. *Nature* **452**, 456–9.

Sharqawy MH, Lienhard JH and Zubair SM (2010) Thermophysical properties of seawater: a review of existing correlations and data. *Desalination and Water Treatment* **16**, 354–80.

Shields GA (2008) Marinoan meltdown. *Nature Geoscience* **1**, 351–3.

Tang H and Chen Y (2013) Global glaciations and atmospheric change at ca. 2.3 Ga. *Geoscience Frontiers* **4**, 583–96.

Tewari HC, Rajendra Prasad B and Kumar P (2018) Global and Indian scenario of crustal thickness. In *Structure and Tectonics of the Indian Continental Crust and Its Adjoining Region, Second Edition* (eds HC Tewari, B Rajendra Prasad and P Kumar), pp. 211–224. Netherlands: Elsevier.

Toggweiler JR and Samuels B (1995) Effect of Drake Passage on the global thermohaline circulation. *Deep Sea Research Part I: Oceanographic Research Papers* **42**, 477–500.

Waldman R, Somot S, Herrmann M, Sevault F and Isachsen PE (2018) On the chaotic variability of deep convection in the Mediterranean Sea. *Geophysical Research Letters* **45**, 2433–43.

Weiss RF (1970) The solubility of nitrogen, oxygen and argon in water and seawater. *Deep Sea Research and Oceanographic Abstracts* **17**, 721–35.

https://doi.org/10.1017/S0016756820001363 Published online by Cambridge University Press